Bioorganic & Medicinal Chemistry Letters 21 (2011) 6964–6968

Contents lists available at SciVerse ScienceDirect

Bioorganic & Medicinal Chemistry Letters

journal homepage: www.elsevier.com/locate/bmcl

Synthesis and docking study of 2-phenylaminopyrimidine Abl tyrosine kinase inhibitors

Shuang Lü, Qun Luo, Xiang Hao, Xianchan Li, Liyun Ji, Wei Zheng, Fuyi Wang *

The CAS Key Laboratory of Analytical Chemistry for Living Biosystems, Beijing National Laboratory for Molecular Sciences, Institute of Chemistry, Chinese Academy of Sciences, Beijing 100190, China

ARTICLE INFO

Article history:
Received 11 May 2011
Revised 22 September 2011
Accepted 30 September 2011
Available online 7 October 2011

Keywords:
Abl kinase
Imatinib analogs
Synthesis
Docking analysis
Virtual screening

ABSTRACT

Six analogs of imatinib, an Abl kinase inhibitor clinically used as a first-line therapeutic agent for chronic myeloid leukaemia (CML), have been synthesized and characterized. And their potency as Abl kinase inhibitors have been screened by a robust virtual screening method developed based on the crystal structure (PDB code 2hyy) of Abl-imatinib complex using Surflex-Docking. The docking results are consistent with the inhibitory potency of the compounds characterized by MS method. And the H-bonds between imatinib analogs and Thr315 and Met318 residues in Abl kinase are shown to be crucial for achieving accurate poses and high binding affinities for the ATP-competitive kinase inhibitors.

The Abl kinase is normally regulated by an autoinhibitory mechanism, the disruption of which leads to chronic myelogenous leukemia (CML).[1] CML is a clonal hematopoietic stem cell disorder characterized by the presence of the Philadelphia (Ph) chromosome. A series of inhibitors with the class of 2-phenylaminopyrimidine (PAP) pharmacophore, in particular imatinib, have been identified to have exceptionally high affinity and specificity for Abl.[2] Imatinib (also named STI-571 or gleevec) is the first protein-tyrosine kinase inhibitor that is used to treat CML clinically. Imatinib displaces ATP and captures a specific inactive conformation of the activation loop of Abl in which the loop mimics bound peptide substrate.[1,3–5] This feature of imatinib could reduce the toxicity to normal cell, but develop drug-resistance due to the Abl kinase domain mutations.[6] To circumvent this problem, rational design of novel inhibitors exhibiting effectiveness against Bcr-Abl has attracted increasing interest. Nilotinib (also named AMN107) is a high affinity aminopyrimidine-based ATP-competitive inhibitor that exhibits superior potency to imatinib as an inhibitor of wild-type Bcr-Abl and imatinib-resistant Bcr-Abl mutant-expressing cells in vitro.[7,8] Katsoulas et al.[9] developed a novel group of dual targeted agent termed 'combi-molecules' capable of not only blocking the Abl kinase active pocket but also damaging DNA, of which ZRF1 was the first ever multitargeted combi-molecule exerting a tandem targeting of Bcr-Abl mediated antiapoptotic signaling and activation of the DNA damage response pathway. A series of potent dual Src/Abl kinase inhibitors based on a 9-(arenethenyl)purine core have been synthesized, and several compounds exhibited modest cellular potency (IC_{50} = 300–400 nM) against the Bcr-Abl mutant T315I that is encouraging given the insensitivity of this mutant to all currently marketed first- and second-generation Bcr-Abl inhibitors.[10]

On the other hand, with the understanding on the interactions of drug candidates and kinases, increasing attention has been paid to develop virtual screening (VS) for avoiding lots of tedious synthetic works for pursuing novel kinase inhibitors as potential anticancer agents. VS, especially docking methodology, is an evolving challenge and an attractive research proposition.[11] However, it still needs to be studied in depth and transformed into a tool of greater confidence and utility. Desiraju and co-workers[12] carried out a VS study on 128 selected inhibitors of epidermal growth factor receptor (EGFR) kinase with GOLD and LigandFit. And Wang et al.[13] tested 100 protein–ligand complexes to evaluate the abilities of eleven popular scoring functions to reproduce experimentally determined structures and binding affinities. The availability of the crystal of Abl complexes with imatinib facilitates the computationally structure-based design of inhibitors against this target.[3,5] Juan et al. established robust 3D-QSAR model for Bcr-Abl inhibitors, and revealed novel insights towards inhibition of Bcr-Abl oncoprotein, providing rational insights into the ligand structural requirements to achieve better Bcr-Abl inhibitory activity which can be utilized in the design of new and more potent Bcr-Abl inhibitors.[14] However, arriving at the appropriate docking/scoring combination is still a challenge because of lacking certain and clear

* Corresponding author. Tel./fax: +86 10 62529069.
E-mail address: fuyi.wang@iccas.ac.cn (F. Wang).

0960-894X/$ - see front matter © 2011 Elsevier Ltd. All rights reserved.
doi:10.1016/j.bmcl.2011.09.127

relationship between docking and ranking accuracies.[15] In this present work, we have established a molecular model based on the crystal structure of Abl-imitanib complex and developed a robust VS method using the Surflex-Docking module for rapid screening of imatinib analogs synthesized in our laboratory. The docking analysis revealed that the formation of two hydrogen bonds between the ligands and the kinase are essential for inhibitory activity, providing rational concepts for the design and synthesis of novel Abl inhibitors.

Firstly, benzoyl chloride intermediates **1b**, **2b**, **3b**, **4b**, **5b** and **6b** were synthesized by reacting respective benzoic acids (**1a**–**5a**, Scheme 1) or picolinic acid (**6a**, Scheme 1) with thionyl chloride. In general, 1 g of benzoic acid compounds **1a**, **2a**, **3a**, **4a**, **5a** or picolinic acid (**6a**) was added to thionyl chloride (12 mL) and then stirred with addition of 50 μL pyridine as a catalyst. The resulting mixture was refluxed until no gas overflowed. Then the excess thionyl chloride was removed off in vacuo, and the residue was directly used for the next step synthesis.

The imatinib analogs 3,4-R_1,R_2-N-(4-methyl-3(4-(pyridine-3-yl)pyrimidin-2-ylamino)phenyl)benzamide ($R_1 = R_2 = H$ (**1**); $R_1 = H$, $R_2 = SCH_3$ (**2**); $R_1 = NO_2$, $R_2 = H$ (**3**); $R_1 = NH_2$, $R_2 = H$ (**4**); $R_1 = R_2 = NO$ (**5**)) and N-(4-methyl-3-(4-(pyridin-3-yl) pyrimidin-2-ylamino)phenyl)picolinamide (**6**) was synthesized following a modified procedure described in the literature[16] as shown in Scheme 1. Briefly, an excess amount of benzoyl chloride compound **1b**, **2b**, **3b**, **4b**, **5b** or **6b** was added to a suspension of 6-methyl-N-(4-(pyridin-3-yl)pyrimidin-2-yl) benzene-1,3-diamine (0.5 g, 2 mmol) in dichloromethane (10 mL) containing TEA (0.58 mL, 4 mmol), and the mixture was reacted at 0 °C for 4 h, and TLC of reaction mass indicated the absence of starting compound. The solution was then filtered and washed with dichloromethane, the excess dichloromethane was removed in vacuo, and the residue was purified by recrystallization from ethanol.

N-(4-methyl-3(4-(pyridine-3-yl)pyrimidin-2-ylamino) phenyl)benzamide (1): ^{1}H NMR (400 MHz, DMSO-d_6): 10.190 (s, 1H), 9.266 (s, 1H), 8.954 (s, 1H), 8.673 (s, 1H), 8.458 (d, 2H), 8.082 (s, 1H), 7.938 (m, 2H), 7.471 (m, 5H), 7.416 (s, 1H), 7.189 (d, 1H), 2.215 (s, 3H, –CH_3); ^{13}C NMR (600 MHz, DMSO-d_6) δ: 165.77, 161.98, 161.56, 159.84, 151.75, 148.57, 138.19, 137.54, 135.48, 134.78, 132.59, 131.80, 130.41, 128.72, 127.98, 124.14, 117.60, 117.13, 107.90, 18.02; MS (ESI, *m/z*): 382.3 ($M+H^+$, $C_{23}H_{20}N_5O$ requires 382.4), 404.3 ($M+Na^+$), 420.3 ($M+K^+$); mp: 190–191 °C; Anal. Calcd for $C_{23}H_{19}N_5O$: C, 72.42; H, 5.02; N, 18.36. Found: C, 71.86; H, 4.97; N, 18.18.

3-(sulfurmethyl)-N-(4-methyl-3(4-(pyridine-3-yl)pyrimidin -2-ylamino)phenyl)benzamide (2): ^{1}H NMR (400 MHz, DMSO-d_6): 10.160 (s, 1H), 9.300 (s, 1H), 8.996 (s, 1H), 8.713 (d, 1H), 8.543–8.492 (m, 2H), 8.100 (s, 1H), 7.951 (d, 2H), 7.600–7.511 (m, 2H), 7.494 (d, 1H), 7.412 (d, 2H), 7.237 (d, 1H), 2.525 (s, 3H, –SCH_3), 2.245 (s, 3H, –CH_3); ^{13}C NMR (600 MHz, DMSO-d_6) δ: 165.19, 161.07, 160.09, 159.67, 145.65, 143.35, 143.02, 141.87, 137.61, 137.58, 135.12, 131.25, 130.54, 128.59, 127.85, 126.91, 125.25, 117.65, 117.46, 108.28, 17.94, 14.54; MS (ESI, *m/z*): 428.5 ($M+H^+$, $C_{24}H_{22}N_5OS$ requires 428.5), 450.5 ($M+Na^+$); mp: 185–186 °C; Anal. Calcd for $C_{24}H_{21}N_5OS{\cdot}3HCl$: C, 53.69; H, 4.51; N, 13.04. Found: C, 55.95; H, 4.78; N, 12.88.

4-nitro-N-(4-methyl-3(4-(pyridine-3-yl)pyrimidin-2-ylamino)phenyl)benzamide (3): ^{1}H NMR (400 MHz, DMSO-d_6): 10.590 (s, 1H), 9.430 (d, 1H), 9.155 (s, 1H), 8.918 (d, 1H), 8.875 (d, 1H), 8.592 (d, 1H), 8.339 (d, 2H), 8.196 (d, 2H), 8.160 (s, 1H), 7.910 (m, 1H), 7.543 (d, 1H), 7.457 (d, 1H), 7.224 (d, 1H), 2.234 (s, 3H, –CH_3); ^{13}C NMR (600 MHz, DMSO-d_6) δ: 164.17, 161.02, 160.08, 159.68, 149.44, 145.27, 142.65, 141.76, 141.02, 137.72, 137.16, 135.12, 130.60, 129.76, 128.27, 126.94, 123.79, 117.54, 117.46, 108.40, 18.01; MS (ESI, *m/z*): 427.2 ($M+H^+$, $C_{23}H_{19}N_6O_3$ requires 427.4), 449.2 ($M+Na^+$); mp: 237–238 °C; Anal. Calcd for $C_{23}H_{18}N_6O_3{\cdot}HCl$: C, 59.68; H, 4.14; N, 18.16. Found: C, 59.29; H, 4.12; N, 17.85.

4-amino-N-(4-methyl-3(4-(pyridine-3-yl)pyrimidin-2-ylamino)phenyl)benzamide (4): ^{1}H NMR (400 MHz, DMSO-d_6): 9.303 (s, 1H), 8.722 (s, 1H), 8.652 (s, 1H), 8.480 (d, 3H), 8.290 (d, 3H), 8.043 (t, 4H), 7.460 (s, 1H), 7.231 (s, 1H), 7.196 (d, 1H), 7.097 (s, 1H), 2.381 (s, 3H, –CH_3); ^{13}C NMR (600 MHz, DMSO-d_6) δ: 164.07, 162.00, 161.51, 159.84, 151.76, 149.46, 148.57, 141.11, 138.30, 137.06, 134.78, 132.56, 130.53, 129.53, 128.48, 124.15, 123.90, 117.57, 117.15, 107.99, 18.05; MS (ESI, *m/z*): 397.3 ($M+H^+$, $C_{23}H_{20}N_6O$ requires 396.4), 419.2 ($M+Na^+$), 435.3 ($M+K^+$); mp: 238–239 °C. Anal. Calcd for $C_{23}H_{20}N_6O{\cdot}HCl$: C, 63.81; H, 4.89; N, 19.41. Found: C, 63.05; H, 4.30; N, 19.14.

3,4-dinitroso-N-(4-methyl-3(4-(pyridine-3-yl)pyrimidin-2-ylamino)phenyl)benzamide (5): ^{1}H NMR (400 MHz, DMSO-d_6): 10.585 (s, 1H), 9.360 (s, 1H), 9.092 (s, 1H), 8.762 (d, 2H), 8.674 (d, 1H), 8.564 (d, 1H), 8.179 (m, 3H), 7.684 (d, 1H), 7.492 (m, 2H), 7.246 (d, 1H), 2.250 (s, 3H, –CH_3); ^{13}C NMR (600 MHz, DMSO-d_6) δ: 164.84, 162.09, 161.62, 159.96, 155.64, 154.26, 151.86, 148.68, 138.37, 137.36, 136.43, 134.89, 132.66, 130.62, 129.34, 128.42, 124.25, 121.77, 121.14, 117.62, 117.17, 108.06, 18.15; MS (ESI, m/z): 440.1 ($M+H^+$, $C_{23}H_{18}N_7O_3$ requires 439.4); mp: 231–233 °C; Anal. Calcd for $C_{23}H_{17}N_7O_3{\cdot}HCl$: C, 58.05; H, 3.81; N, 20.60. Found: C, 58.20; H, 3.85; N, 20.92.

N-(4-methyl-3-(4-(pyridin-3-yl)pyrimidin-2-ylamino) phenyl)picolinamide (6): ^{1}H NMR (400 MHz, DMSO-d_6): 10.566 (s, 1H), 9.281 (s, 1H), 8.987 (s, 1H), 8.744 (d, 1H), 8.688 (d, 1H), 8.527–8.477 (m, 2H), 8.256 (s, 1H), 8.163 (d, 1H), 8.089 (t, 1H), 7.678 (m, 1H), 7.580–7.507 (m, 2H), 7.446 (d, 1H), 7.234 (d, 1H), 2.245 (s, 3H, –CH_3); ^{13}C NMR (600 MHz, DMSO-d_6) δ: 158.58, 136.73, 136.55,

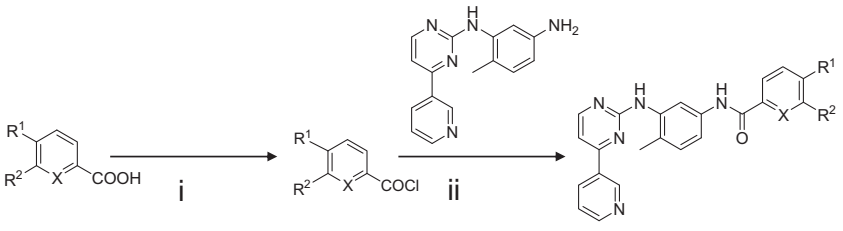

1a X=C R^1= R^2=H
2a X=C R^1=H R^2=SCH_3
3a X=C R^1=NO_2 R^2=H
4a X=C R^1=NH_2 R^2=H
5a X=C R^1= R^2=NH_2
6a X=N R^1= R^2=H

1b X=C R^1= R^2=H
2b X=C R^1=H R^2=SCH_3
3b X=C R^1=NO_2 R^2=H
4b X=C R^1=NH_2 R^2=H
5b X=C R^1= R^2=NH_2
6b X=N R^1= R^2=H

1 X=C R^1= R^2=H
2 X=C R^1=H R^2=SCH_3
3 X=C R^1=NO_2 R^2=H
4 X=C R^1=NH_2 R^2=H
5 X=C R^1= R^2=NH_2
6 X=N R^1= R^2=H

Scheme 1. Synthesis route of imatinib analogs. (i) $SOCl_2$, py, N_2, rt, 70 °C; (ii) CH_2Cl_2, Et_3N, 0 °C, 4 h.

132.88, 131.44, 130.80, 130.07, 128.53, 126.56, 126.16, 125.44, 114.50, 56.05, 49.65; MS (ESI, *m/z*): 383.1 ($M+H^+$, $C_{22}H_{19}N_6O$ requires 382.4); mp: 192–193 °C; Anal. Calcd for $C_{22}H_{18}N_6O$: C, 69.10; H, 4.74; N, 21.98. Found: C, 68.68; H, 4.68; N, 21.35.

Crystal of compound **1** was grown from its saturated DMF solution at 4 °C. The single-crystal X-ray diffraction analysis reveals that **1** crystallizes in the monoclinic $P2_1/n$ space group (Fig. 1).[17] In the crystal, we observed two intermolecular hydrogen bonds: N(4)-H(4A)···N(1) and N(5)-H(5A)···N(3) (Fig. S1 in Supplementary data) and the bond distances were 2.931 and 3.041, respectively. And estimated interplane distance between the phenyl rings of the two molecules is about 3.37 Å, thus the compound in crystal shows extensive intermolecular π···π interactions (Fig. S2). The dihedral angels between the pyrimidine and the pyridine rings, the pyrimidine and the neighboring benzene, and the pyrimidine and the rightmost benzene were calculated to be 3.53°, 71.67° and 89.05°, respectively. Standard data relating to the X-ray crystal structure of compound **1** have been deposited in the Cambridge Crystallographic Data Centre with CCDC reference number 845049.

We have previously developed a mass spectrometric approach to evaluate the inhibitory potency of imitanib derivative compounds **1**–**6**.[18] Given that the inhibitory efficiency of 10 μM imatinib towards Abl was 100%, the relatively inhibitory efficiency of compounds **1**–**6** at the same concentration was determined to be 34.3, 74.9, 20.0, 19.9, 16.3 and 0, respectively. And the IC_{50} values of imitanib and the derivative compounds **1**, **2** and **5** against Abl are 0.234, 12.7, 1.1 and >25 μM, respectively.

The docking analysis was performed using the Surflex-Dock module, a fully automatic docking tool available on SYBYL version X 1.1 (Tripos Inc.), running on Dual-core Intel(R) E5300 CPU 2.60 GHz, RAM Memory 2 GB under the Windows XP system. The crystal structure of Abl-imatinib complex was collected from PDB under code 2hyy.[19] All the hydrogen atoms were added to define the correct configuration and tautomeric states. With standard set parameters, then the modeled structure was energy-minimized using AMBER7 F99 force field with the Powell energy minimization algorithm, distance dependent dielectric function and current charges. After extracted the bound ligand imatinib, the structure of Abl kinase corresponding to the constringent energy gradient (0.05 kcal mol^{-1}) was used for re-docking and scoring calculations of imatinib so as to check the accuracy of the Surflex-Dock program.

For a direct docking, for which no any configuration restraints are set up, the re-docking score and RMSD value for the Abl-imatinib complex were 10.66 and 2.29, respectively. It can be seen that the pyrimidine ring and pyridine ring of the docking ligand molecule were superposed with those of the ligand in the Abl-imatinib complex crystal, but the rest was deviated from the original position (Figs. S3 and S4). The docking molecule bound to Abl via three H-bond interactions: the pyridine-N with the backbone-NH of Met318, the anilino-NH with the side chain of Thr315, the amide-NH to the side chain of Glu286, but there were lack of three H-bonds observed in the X-ray crystal structure of Abl-imatinib complex (Figs. S3 and S4), indicating that the direct docking is not effective. The reason may be that we did not consider the protonation of the nitrogen of *N*-methylpiperazine in the ligand. Taking the protonation into account, a significant improvement was observed for an indirect docking. The position of the docking molecule was completely overlapped with that of the ligand in the Abl-imatinib complex crystal, and the number and location of the H-bonds between the docking ligand and the receptor were the same as those of the ligand in the complex crystal (Fig. 2). The docking score and RMSD value were 13.08 and 0.39, respectively, indicative of that the indirect docking results upon the protonation of the ligand was more reasonable and accurate than that of the direct docking.

Then the six imatinib analogs, of which the structures were built in SYBYL and minimized by Tripos force field with an energy convergence value of 0.05 kcal mol^{-1}, were separately docked into the binding pocket for docking-scoring calculations using the same method validated. The docking scores are 11.20 (**1**), 12.10 (**2**), 8.72 (**3**), 9.41 (**4**), 6.51 (**5**) and 5.99 (**6**), respectively. These results are consistent with the inhibitory potency order of the compounds characterized by MS method, that is, the higher the score of the compound, the higher its inhibitory efficiency.[18]

Further analysis on the interactions between Abl and compounds **1** and **2** shows that these two compounds make three hydrogen bonds with the receptor: the pyridine-N with the backbone-NH of Met318, the anilino-NH with the side chain of Thr315, the amide-NH to the side chain of Glu286, but both lack of two H-bonds which form between the *N*-methylpiperazine of imatinib and the carboxyl of Ile360 and His361 residues, due to the substitution of piperazine by benzene (for **1**) or sulfurmethylbenzene (for **2**). The leftmost part of compounds **1** and **2** overlapped with imatinib, and the amide-carbonyl of **1** and **2** shifted away from Asp381, leading to absence of the H-bond between the amide-carbonyl group and amide-NH of Asp381 (Fig. 3). The presence of Thr315 appears to be a key requirement for the ability of this class of compounds to inhibit wild-type Abl. This threonine residue is replaced by a methionine residue in many protein kinases, for example, insulin receptor tyrosine kinase (IRK). Methionine residues cannot form this kind of hydrogen bond with imatinib ligand, and its side chain would also interfere with the binding of the phenyl-moiety of imatinib, but not affect the binding of ATP.

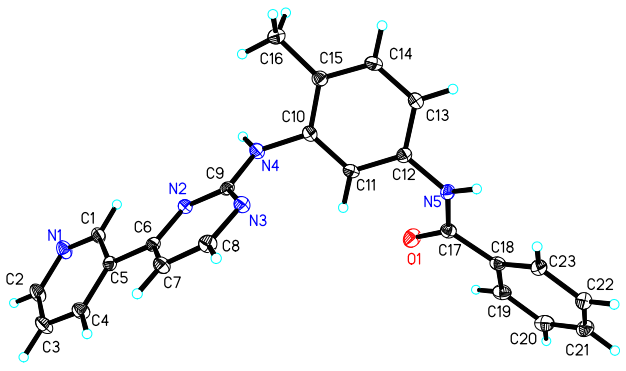

Figure 1. A view of compound **1** with displacement ellipsoids drawn at the 30% probability level.

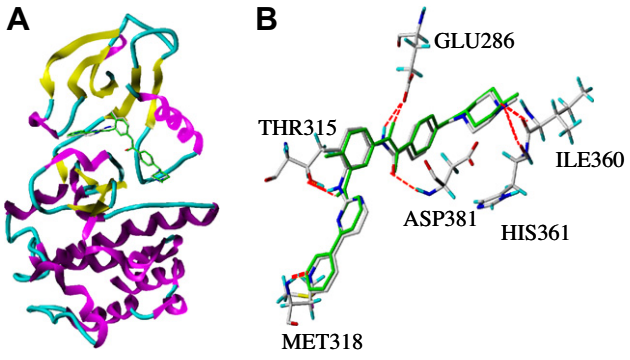

Figure 2. (A) The superposition of the bound imatinib (green) to Abl in the crystal structure[3,5] and docked imatinib (colored by atoms) to Abl in the molecular model constructed by indirect docking. (B) Details of potential hydrogen bonds (red dotted lines) between imatinib and Abl generated by indirect docking analysis.

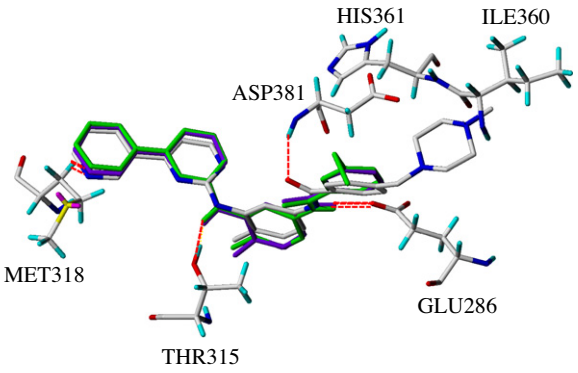

Figure 3. Detail of the binding of compounds **1** and **2** to Abl showing potential hydrogen bonds in red dotted lines. The ligands colored by atoms, in purple and in green represent imatinib in Abl-imatinib complex crystal and docking compounds **1** and **2**, respectively.

This may be the reason why the kinases with Met residue in the place of Thr315 in the ATP-binding pocket are resistant to imatinib. However, the formation of H-bond between imatinib derivatives and Met318 of Abl kinase strengthens the binding of the ligands to Abl. The adenine group of ATP generally makes two H-bonds with backbone atoms of the peptide chain connecting the N- and C-lobes of kinase domains. The extracyclic amino group of ATP donates a hydrogen bond to the carbonyl oxygen of the residue corresponding to Glu316 in Abl, and the nitrogen (N1) of the purine ring accepts a hydrogen bond from the amide nitrogen of residue Met318.[5,20] Many small molecular inhibitors of protein kinases are anchored to the kinase domain by the pair of hydrogen bonds that mimic those formed by adenine.

The pattern of hydrogen bonds formed by compound **3** with the Abl receptor is similar to that of compounds **1** and **2** with Abl kinase. The carbonyl oxygen deviated from the Asp-Phe-Gly (DGF) motif in Abl and accepted a hydrogen bond from the amide nitrogen of residue Lys271 which replaced the residue Asp381 (Fig. S5). Compounds **4**, **5** and **6** had many similarities to each another: deviation from the original position of imatinib in the C-lobe of Abl, and accepting hydrogen bond from residue Tyr253. Notably, compound **6** lost the two important H-bonds formed with Thr315 and Met318 residues (Figs. S6–S8), leading it to be the weakest inhibitor to Abl as indicated by both docking analysis and MS-based assay.[18]

We also compared the conformational differences of compound **1** between the docking molecule in the Abl using Surflex-Docking and the molecule in the crystal structure (Fig. 1). We first kept the possibility of H-bonding between the N4···H of compound **1** and the side chain of Thr315 because of the importance of this hydrogen bond. The molecular model (Fig. 4) showed that when we overlapped the pyrimidine ring of the two molecules, the rest of the docking molecule deviated from the crystal conformation to meet the requirements for docking into the ATP-binding pocket. The dihedral angel between the pyrimidine and the pyridine rings changed from 3.53° to 14.93°, while the other two dihedral angels changed little. And the position of the two benzene rings in the docking molecule deviated from the original position towards the wall of the active pocket. These imply that the conformation of the kinase inhibitors can be induced to fit the binding to the ATP-pocket in the Abl kinase.

In summary, with the protonation of the nitrogen of *N*-methylpiperazine in Abl kinase inhibitor imatinib as a restraint, the present work demonstrates that Surflex-Docking provides a robust and accurate virtual screening method for rational design of PTK inhibitors as potential anticancer agents. The docking-scores for the newly synthesized imatinib analogs are consistent with the inhibitory potency of the compounds characterized by MS method. Furthermore, the molecular models constructed by docking analysis indicate that the formation of ligand-receptor hydrogen bonds between the py-N and Met318, and the anilino N–H and Thr315 are crucial to achieve accurate poses and high binding affinities for the ATP-competitive kinase inhibitors. In particular, the presence of Thr315 in the ATP-binding pocket of the kinases is a key structural requirement for this class of imatinib analogs binding to the receptors. The absence of the H-bond between the docking ligands and the Thr315 in the ATP-binding pocket leads to dramatically reduction of inhibitory activities of the imatinib derivatives. Our findings indicate that the virtual screening method based on Surflex-Docking can provide rational insights to design novel kinase inhibitors for development of next generation of molecular targeting anticancer agents.

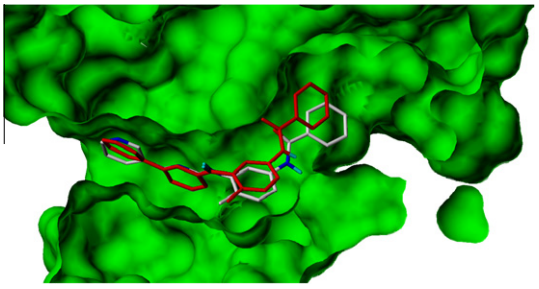

Figure 4. The docked conformers/poses of compound **1** (color by atoms) at the active site of Abl kinase as generated via Surflex docking-scoring combinations compared with the X-ray structure of unbound **1** (red).

Acknowledgments

We thank NSFC (Grant No. 90713020, 20975103, 21005081 (for X.L.) and 21020102039), the 973 Program of MOST (Grant No. 2007CB935601) and the Chinese Academy of Sciences (Hundred Talent Program) for support.

Supplementary data

Supplementary data associated with this article can be found, in the online version, at doi:10.1016/j.bmcl.2011.09.127.

References and notes

1. Nagar, B.; Hantschel, O.; Young, M. A.; Scheffzek, K.; Veach, D.; Bornmann, V.; Clarkson, B.; Superti-Furga, G.; Kuriyan, J. *Cell* **2003**, *112*, 859.
2. Zimmermann, J.; Buchdunger, E.; Mett, H.; Meyer, T.; Lydon, N. B. *Bioorg. Med. Chem. Lett.* **1997**, *7*, 187.
3. Schindler, T.; Bornmann, W.; Pellicena, P.; Miller, W. T.; Clarkson, B.; Kuriyan, J. *Science* **2000**, *289*, 1938.
4. Manley, P. W.; Cowan-Jacob, S. W.; Buchdunger, E.; Fabbro, D.; Fendrich, G.; Furet, P.; Meyer, T.; Zimmermann, J. *Eur. J. Cancer* **2002**, *38*, S19.
5. Nagar, B.; Bornmann, W. G.; Pellicena, P.; Schindler, T.; Veach, D. R.; Miller, W. T.; Clarkson, B.; Kuriyan, J. *Cancer Res.* **2002**, *62*, 4236.
6. Blagosklonny, M. V. *Leukemia* **2002**, *16*, 570.
7. Weisberg, E.; Manley, P.; Mestan, J.; Cowan-Jacob, S.; Ray, A.; Griffin, J. D. *Br. J. Cancer* **2006**, *94*, 1765.
8. Weisberg, E.; Manley, P. W.; Breitenstein, W.; Bruggen, J.; Cowan-Jacob, S. W.; Ray, A.; Huntly, B.; Fabbro, D.; Fendrich, G.; Hall-Meyers, E.; Kung, A. L.; Mestan, J.; Daley, G. Q.; Callahan, L.; Catley, L.; Cavazza, C.; Mohammed, A.; Neuberg, D.; Wright, R. D.; Gilliland, D. G.; Griffin, J. D. *Cancer Cell* **2005**, *7*, 129.
9. Katsoulas, A.; Rachid, Z.; McNamee, J. P.; Williams, C.; Jean-Claude, B. J. *Mol. Cancer Ther.* **2008**, *7*, 1033.
10. Huang, W. S.; Zhu, X. T.; Wang, Y. H.; Azam, M.; Wen, D.; Sundaramoorthi, R.; Thomas, R. M.; Liu, S.; Banda, G.; Lentini, S. P.; Das, S.; Xu, Q. H.; Keats, J.; Wang, F.; Wardwell, S.; Ning, Y. Y.; Snodgrass, J. T.; Broudy, M. I.; Russian, K.; Daley, G. Q.; Iuliucci, J.; Dalgarno, D. C.; Clackson, T.; Sawyer, T. K.; Shakespeare, W. C. *J. Med. Chem.* **2009**, *52*, 4743.
11. Keseru, G. M. *J. Comput. Aided Mol. Des.* **2001**, *15*, 649.
12. Aparna, V.; Rambabu, G.; Panigrahi, S. K.; Sarma, J.; Desiraju, G. R. *J. Chem. Inf. Model.* **2005**, *45*, 725.
13. Wang, R. X.; Lu, Y. P.; Wang, S. M. *J. Med. Chem.* **2003**, *46*, 2287.

14. Juan, A. A. S. *J. Mol. Graphics Modell.* **2007**, *26*, 482.
15. Bissantz, C.; Folkers, G.; Rognan, D. *J. Med. Chem.* **2000**, *43*, 4759.
16. Liu, Y. F.; Wang, C. L.; Bai, Y. J.; Han, N.; Jiao, J. P.; Qi, X. L. *Org Process Res. Dev.* **2008**, *12*, 490.
17. Crystal data for **1**: $C_{23}H_{19}N_5O$, $M = 381.43$, monoclinic, space group $P2_1/n$, $a = 8.0283(16)$ Å, $b = 15.129(3)$ Å, $c = 16.088(3)$ Å, $V = 1948.3(7)$ Å^3, $Z = 4$, Dc = 1.300 mg/m^3, F(000) = 800, crystal dimensions $0.46 \times 0.42 \times 0.36$ mm, $R_1 = 0.0528$, $wR_2 = 0.1030$ for 3428 reflections with $I > 2\sigma(I)$, GOF = 1.153, largest peak/hole 0.233/−0.238.
18. Lü, S.; Luo, Q.; Li, X. C.; Wu, J. H.; Liu, J. A.; Xiong, S. X.; Feng, Y. Q.; Wang, F. Y. *Analyst* **2010**, *135*, 2858.
19. Cowan-Jacob, S. W.; Fendrich, G.; Floersheimer, A.; Furet, P.; Liebetanz, J.; Rummel, G.; Rheinberger, P.; Centeleghe, M.; Fabbro, D.; Manley, P. W. *Acta Crystallogr., Sect. D* **2007**, *63*, 80.
20. Zheng, J. H.; Knighton, D. R.; Teneyck, L. F.; Karlsson, R.; Xuong, N. H.; Taylor, S. S.; Sowadski, J. M. *Biochemistry (Mosc)* **1993**, *32*, 2154.